Optics Communications 323 (2014) 110–118

Contents lists available at ScienceDirect

Optics Communications

journal homepage: www.elsevier.com/locate/optcom

Two-step spatial phase-shifting lateral shearing interferometry by triple gratings

Zhenyan Guo, Yang Song*, Jia Wang, Zhenhua Li, Anzhi He

Department of Information Physics and Engineering, Nanjing University of Science and Technology, Nanjing 210094, China

ARTICLE INFO

Article history:
Received 5 November 2013
Received in revised form
27 January 2014
Accepted 21 February 2014
Available online 11 March 2014

Keywords:
Linear gratings
Phase shift
Frequency filtering
Phase retrieval
Tomographic image processing
Moiré techniques

ABSTRACT

To acquire phase projection information for moiré tomography, a new spatial phase-shifting lateral shearing interferometry is presented in this paper. The system is very simple and contains only three linear gratings and two filters. No wave plates or polarization elements are introduced. Moreover, via using a 4-f system, the optical path is greatly shortened and two complete spatial phase-shifted lateral shearing interferograms can be obtained simultaneously. A corresponding two-step phase-shifting algorithm is used for phase retrieval and the interferometry is used to extract the first-order partial derivative of the spherical wave. The results show that the proposed method is not only feasible but also has high accuracy. Propane flame phase information is measured by the optical system. Finally, error analysis of phase projection extracted by two-step spatial phase-shifting method is mathematically conducted.

1. Introduction

Advantages of nonintrusiveness, instantaneity, and 3D reconstruction has made optical computerized tomography (OCT) a powerful tool for quantitatively measuring the 3D physical parameters of flow fields [1–6]. OCT is a combination of computerized tomography and optical methods such as interferometry, holographic interferometry, and moiré deflectometry. Compared with interferometry and holographic interferometry, moiré deflectometry is more competitive since it requires simple devices, features a wide measurement range, and has low mechanical stability requirements. Therefore, moiré deflectometry is more suitable in noisy environments than other techniques for complex flow field diagnosis, such as flame field diagnosis [7,8], supersonic flow field diagnosis [9,10], and plasma field diagnosis [11,12].

Projection information extraction is critical in moiré tomography. Many approaches have been studied to achieve this extraction such as the fringe detection method, Fourier transform method, and phase-shift method. Among the fringe detection methods, the moiré fringe is processed based on image intensity. Vlad et al. performed real-time data acquisition and completed the quantitative interpretation of a moiré fringe following simple algorithms associating computer image processors [13]. Subsequently, Servin et al. presented an algorithm for automatic fringe detection applied to moiré deflectometry [14]. Despite the successes of these studies, however, all of the methods were used to extract the fringe skeleton information and interpolated other values of the fringe pattern, which indicates that measurement of the field with the demand of high accuracy is not satisfied. Using Fourier transform methods, Wang [15] applied Fourier transform evaluation for moiré deflectograms to automatically map the temperature field based on the processing of fringe patterns in the frequency domain. Quiroga et al. [16] analyzed the grid moiré deflectograms produced by squared gratings using the Fourier transform method. Recently, Sun et al. extracted the partial derivative of phase projection in two perpendicular directions of crossed gratings based on Fourier transform method and performed 3D volume computerized tomography reconstruction [7].

The phase-shift methods have been considered as other essential techniques to obtain phase information from fringe patterns. With respect to Fourier transform methods, the phase-shift methods only employ simple arithmetic operations to the fringe patterns in spatial domain which indicates the computation complexity is reduced and easier to implement. The phase-shift methods contain temporal phase-shift methods and spatial phase-shift methods.

However, temporal phase-shift methods require to obtain several phase-shifted fringe patterns sequentially such as via laterally moving a grating to acquire the phase-shifted moiré fringe patterns [17]. Thus, temporal phase-shift methods can only be applied in measuring stable fields [18] and are not suitable for measuring rapidly varying flow fields. Compared with temporal phase-shift methods, spatial phase-shift methods are more useful for diagnosing rapidly changing objects because they can obtain several phase-shifted interferograms

* Corresponding author.
E-mail addresses: guozhenyan15@163.com (Z. Guo), sy0204@mail.njust.edu.cn (Y. Song).

http://dx.doi.org/10.1016/j.optcom.2014.02.057
0030-4018

simultaneously. The spatial phase-shifting with spectroscopes and polarization technique systems are introduced to measure the surface figure [19]. Xie et al. implemented the spatial phase shift using Fourier transform based on the Michelson interferometer which can be used to measure the relative deformation of object surface quantitatively [20]. Generally, in order to get several spatial phase-shifted fringe patterns simultaneously, gratings play an important role in the spatial phase-shifted optical configurations. Linear gratings were applied to create the desired phase-shifted interferograms in different diffraction orders by Kwon [21]. Rodriguez-Zurita et al. [22] placed a crossed grating in the spectrum of a 4-f system to generate several patterns and used polarization elements to generate the desired phase-shifting. Using this spatial phase-shifting method Toto-Arellano et al. [23] extracted the slope of a phase object.

We recently derived the moiré fringe patterns produced by double-grating lateral shearing interference from the scalar diffraction theory and obtained the mathematical expressions of the intensities distribution of interferograms [24]. But only one interferogram can be obtained by a pinhole filter at a time. Thus, the spatial phase-shift methods cannot be used to extract the phase information of objects. After detailed derivation, the phase-shift was found between $+1$ and -1 diffraction orders of interferograms [25]; they can be acquired simultaneously by using the splitting character of double gratings. Afterwards, based on the theoretical derivation, three gratings were used to generate four phase-shifted interferograms at the same time and the four-step phase-shifting method was used to extract the phase information [26], but the optical path appears complex. Thus, we use a crossed grating instead of two Ronchi gratings and the optical configuration containing only a crossed grating and a linear grating is proposed. Meanwhile the phase information is extracted by a six-step spatial phase-shifting algorithm [27]. However, the problem encountered in the optical system is the optical path is too long.

The optical configuration takes advantage of the splitting character of gratings to realize the synchronization acquisition of several phase-shifted interferograms. But the gratings diffraction efficiency is low which will cause the longer optical path depending only on the diffraction character of gratings to separate interferograms from each other. Hence, above optical systems are difficult to apply in practice. Taking Ref. [27] for an example, the optical path is shown as Fig. 1. According to the grating equation, we have $d\sin\theta = n\lambda$ $(n=1)$, where d is the gratings period and λ is the wavelength of incident light. Furthermore, according to geometrical relationship, we also have the equation of $tg\theta = \beta F/\Delta_2$, where β is real, F represents the light aperture of the system and βF indicates the distance between double adjacent interferograms. As a result, when θ is small, Δ_2 can be derived as

$$\Delta_2 = \frac{\beta F d}{\lambda}, \quad \beta \geq 1, \tag{1}$$

When the periods d of gratings CG1 and G2, the diameter F of every interferogram, the wavelength λ of incident light and the parameter β is 50 lines/mm, 50 mm, 532 nm and 1, respectively, Δ_2 will be calculated to be about 1.8 m by Eq. (1). Thus, the optical path length is too large to apply in practice. What is more, the additional higher-order partial derivative (the derivative in x or y direction) of the phase projections cannot be eliminated. In Ref. [27], the intensity distribution of each interferogram is written as

$$\begin{aligned}
I_1(x,y) &= 2a_1^4a_0^2\left\{1+\cos\left[\frac{4\pi}{d}\sin\frac{\alpha}{2}y + kP1 - \xi' + \eta' - \frac{2\pi b}{d}\right]\right\}\\
I_2(x,y) &= 2a_1^2a_0^4\left\{1+\cos\left[\frac{4\pi}{d}\sin\frac{\alpha}{2}y + kP1 + \eta' - \frac{2\pi b}{d}\right]\right\}\\
I_3(x,y) &= 2a_1^4a_0^2\left\{1+\cos\left[\frac{4\pi}{d}\sin\frac{\alpha}{2}y + kP1 + \xi' + \eta' - \frac{2\pi b}{d}\right]\right\}\\
I_4(x,y) &= 2a_1^4a_0^2\left\{1+\cos\left[\frac{4\pi}{d}\sin\frac{\alpha}{2}y + kP1 - \xi' - \eta' - \frac{2\pi b}{d}\right]\right\}\\
I_5(x,y) &= 2a_1^2a_0^4\left\{1+\cos\left[\frac{4\pi}{d}\sin\frac{\alpha}{2}y + kP1 - \eta' - \frac{2\pi b}{d}\right]\right\}\\
I_6(x,y) &= 2a_1^4a_0^2\left\{1+\cos\left[\frac{4\pi}{d}\sin\frac{\alpha}{2}y + kP1 + \xi' - \eta' - \frac{2\pi b}{d}\right]\right\},
\end{aligned} \tag{2}$$

$$\begin{aligned}
kP1 &= \frac{2\pi}{d}\left(\frac{\partial\varphi(x,y)}{\partial x}\Delta_1\cos\frac{\alpha}{2} - \frac{\partial\varphi(x,y)}{\partial y}(\Delta_1+2\Delta_2)\sin\frac{\alpha}{2}\right)\\
\xi' &= kP2 - 2\pi\beta N\\
\eta' &= kP3 - \frac{\pi\lambda\Delta_1}{d^2},
\end{aligned} \tag{3}$$

$$\begin{aligned}
kP2 &= \pi\lambda\left(\begin{array}{l}\frac{\partial^2\varphi(x,y)}{\partial x}\left[-\frac{2\Delta\Delta_1}{d^2}\sin\frac{\alpha}{2}\cos\frac{\alpha}{2}\right] + \frac{\partial^2\varphi(x,y)}{\partial y}\left[\frac{2\Delta(\Delta_1+2\Delta_2)}{d^2}\cos\frac{\alpha}{2}\sin\frac{\alpha}{2}\right]\\ -2\frac{\partial^2\varphi(x,y)}{\partial x\partial y}\left(\frac{\Delta^2}{d^2}\cos\alpha - \frac{\Delta\Delta_2}{d^2}\right)\end{array}\right)\\
kP3 &= \pi\lambda\left(\begin{array}{l}\frac{\partial^2\varphi(x,y)}{\partial x}\left[\frac{\Delta_1{}^2+2\Delta_1\Delta_2}{d^2}\cos^2\frac{\alpha}{2}\right] + \frac{\partial^2\varphi(x,y)}{\partial y}\left[\frac{\Delta_1{}^2+2\Delta_1\Delta_2}{d^2}\sin^2\frac{\alpha}{2}\right]\\ -2\frac{\partial^2\varphi(x,y)}{\partial x\partial y}\left(\frac{\Delta^2+\Delta_2{}^2}{d^2}\cos\frac{\alpha}{2}\sin\frac{\alpha}{2}\right)\end{array}\right).
\end{aligned} \tag{4}$$

From Eq. (3), we can see if Δ_2 is too large, the partial derivative in y direction $(\partial\varphi(x,y)/\partial y)(\Delta_1+2\Delta_2)\sin(\alpha/2)$ cannot be omitted. But it had been omitted in practical phase retrieve. In addition, in Eq. (4), every higher order partial derivative is modulate by $\Delta_2(\Delta=\Delta_1+\Delta_2)$, which made the coefficients too large to omit the influence of the higher order partial derivative $\partial^2\varphi(x,y)/\partial x$, $\partial^2\varphi(x,y)/\partial y$ and $\partial^2\varphi(x,y)/\partial x\partial y$. But when we calculate the value of phase shift ξ' or η' in the experiment, the values of $KP2$ and $KP3$ are not considered. As a result, the phase retrieval accuracy decreases. Afterwards, a new optical structure containing a 4-f system behind double circular gratings was proposed in which the optical path is greatly shortened and the radial first-order derivative of phase projection is extracted via using double circular gratings [28]. However, as the spectra of circular gratings are circles, in order to separate $+1$ and -1 order spectrum, annular and circular filters are introduced. But the annular filter is hard to manufacture and adjust, which will introduce some errors in the region near optical axis in practical measurement.

In this paper, a new optical configuration containing three linear gratings is presented to avoid disadvantages of the former double circular gratings configuration and the lateral first-order derivative of

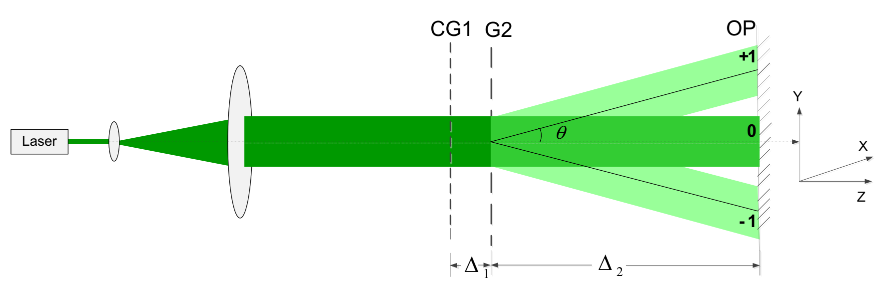

Fig. 1. Optical configuration of a crossed and linear grating interferometer.